AJNR

White Matter Lesions in Panencephalopathic Type of Creutzfeldt-Jakob Disease: MR Imaging and Pathologic Correlations

Eiji Matsusue, Toshibumi Kinoshita, Shuji Sugihara, Shinya Fujii, Toshihide Ogawa and Eisaku Ohama

AJNR Am J Neuroradiol 2004, 25 (6) 910-918
http://www.ajnr.org/content/25/6/910

AJNR Am J Neuroradiol 25:910–918, June/July 2004

White Matter Lesions in Panencephalopathic Type of Creutzfeldt-Jakob Disease: MR Imaging and Pathologic Correlations

Eiji Matsusue, Toshibumi Kinoshita, Shuji Sugihara, Shinya Fujii, Toshihide Ogawa, and Eisaku Ohama

BACKGROUND AND PURPOSE: **A panencephalopathic type of Creutzfeldt-Jakob disease (pCJD) is characterized by the extensive involvement of the cerebral white matter as well as the cerebral gray matter. It has been a point of controversy, however, whether the white matter changes represent primary or secondary degeneration. The aim of this study was to elucidate, by using MR images and histologic examinations, whether the white matter lesions in pCJD are primary or secondary degeneration.**

METHODS: **Serial changes of T2 hyperintensities and histologic findings of six autopsy-proved cases of pCJD were retrospectively analyzed.**

RESULTS: **Serial MR images of brains affected by pCJD revealed that T2 hyperintensities appeared in the cerebral gray matter 2–5 months after onset and in the cerebral white matter around the lateral ventricles approximately 5 months after onset. They rapidly extended to deep and subcortical white matter during the next several months and then to the entire cerebral white matter 10 months after onset. Histologic examination of the white matter lesions revealed spongy changes or tissue rarefaction associated with gemistocytic astrocytosis, which indicates primary involvement of the white matter. At the terminal stages of cases with a longer clinical course, MR images showed T2 hyperintensities in the corticospinal tracts in the internal capsule and brain stem, which histologically disclosed loss of myelin and axons accompanied by fibrillary gliosis that indicates secondary degeneration.**

CONCLUSION: **Cerebral white matter lesions in pCJD were considered to be primary changes of the disease, but the lesions of the corticospinal tracts were secondary to cortical or cerebral or both white matter lesions.**

Creutzfeldt-Jakob disease (CJD), the most common form of human prion disease, primarily affects the gray matter of the brain and occurs in four forms: sporadic, familial, iatrogenic, and a new variant. The sporadic form occurs most frequently. The histologic hallmarks of CJD are spongiform change, neuronal loss, and gemistocytic astrocytosis, as well as abnormal prion protein deposition in the gray matter.

White matter lesions are rare in cases of CJD in North American and European countries and are generally considered to be secondary changes to gray matter lesions (1, 2). In some cases, however, primary involvement of the cerebral white matter, as well as the gray matter, has been suggested (3–9). In 1981, Mizutani et al (10) reported eight Japanese cases of sporadic CJD in which there was primary involvement of the cerebral white matter, as well as the cerebral cortex, and named those cases a panencephalopathic type of CJD (pCJD). It has subsequently been shown that this type of CJD is rather common in Japanese cases of CJD (10–22). Histologic examinations of the cerebral white matter of this type of CJD reveal severe loss of myelin and axons, spongiform changes, or tissue rarefaction accompanied by scattered macrophages and proliferation of gemistocytic astrocytes. Because both spongiform changes and gemistocytic astrocytosis are exceptional features of secondary degeneration, these histologic features indicate primary involvement of the white matter (5, 8–10, 12–15).

Generalized cerebral atrophy and hyperintensities in the basal ganglia on T2-weighted images have been

Received October 6, 2003; accepted after revision December 19.

From the Division of Radiology, Department of Pathophysiological and Therapeutic Science (E.M., T.K., S.S., S.F., T.O.), and the Department of Neuropathology, Institute of Neurological Sciences (E.M., E.O.), Faculty of Medicine, Tottori University, Yonago, Japan.

Address correspondence to Eiji Matsusue, Division of Radiology, Department of Pathophysiological and Therapeutic Science, Faculty of Medicine, Tottori University. 36-1 Nishi-oho, Yonago, Tottori 683-8504, Japan.

Summary of clinical and pathologic findings in six cases of pCJD

					Histologic Findings (gray matter: spongiform change, neuronal loss and gliosis; white matter: loss of myelin and axons)						
Case No.	Age (y)/Sex	Duration of Illness (mo)	Clinical Findings (mo after onset)	Brain Weight (gs)	Cerebral Cortex	Cerebral White Matter	Internal Capsule	Basal Ganglia	Thalamus	Brain Stem	Middle Cerebellar Peduncle
1	66/M	8	Dementia (1); change of character (0); myoclonus (3); ataxia (2); akinetic mutism (4); dysarthria (2); PSD (4)	1210	++	+–++	–	ST: ++ GP: ++	++	CP: – PLF: – PN: – PTF: –	–
2	64/F	15	Dementia (1); ataxia (0); myoclonus (1); tremor (1); akinetic mutism (2); dystonia (1); PSD	900	+++	+++	–	ST: +++ GP: ++	++	CP: – PLF: + PN: – PTF: +	–
3	78/F	22	Dementia (0); tremor (1); myoclonus (2); diplopia (1); akinetic mutism (3); PSD (2)	740	+++	+++	–	ST: +++ GP: +++	++–+++	CP: – PLF: – PN: + PTF: ++	++
4	76/F	25	Dementia (2); tremor (0); myoclonus (2); hemiplegia (1); akinetic mutism (3); PSD	720	+++	+++	–	ST: +++ GP: ++	++–+++	CP: + PLF: + PN: + PTF: ++	+
5	68/F	28	Dementia (1); ataxia (0); myoclonus (2); chorea (1); akinetic mutism (2); PSD	650	+++	+++	++	ST: +++ GP: ++	++–+++	CP: +++ PLF: +++ PN: +++ PTF: +++	+++
6	82/F	30	Dementia (0); gait disturbance (5); myoclonus (5); akinetic mutism (6); PSD	740	+++	+++	++	ST: +++ GP: ++	++–+++	CP: +++ PLF: +++ PN: +++ PTF: +++	+++

Note.—PSD, periodic synchronous discharge on electroencephalogram; ST, striatum; GP, globus pallidus; CP, cerebral peduncle; PN, pontine nucleus; PTF, pontine transverse fibers; PLF, pontine longitudinal fibers; +, mild; ++, moderate; +++, marked.

established as characteristic MR findings of sporadic CJD (23–25). Diffusion-weighted imaging (DWI) and fluid-attenuated inversion recovery (FLAIR) imaging have been reported to be more sensitive in the early stages, showing hyperintensities in both the cerebral cortex and the basal ganglia (26–29). To our knowledge, this is the first MR study describing hyperintensities on FLAIR or DWI images in the cerebral white matter in patients with pCJD, although a few MR studies have described T2 hyperintensities in the cerebral white matter in those patients (7, 18, 22).

To ascertain whether white matter changes in cases of pCJD reflect primary or secondary degeneration, we analyzed serial changes of hyperintensities in the white matter on T2-weighted MR images in six autopsy-proved Japanese cases of pCJD. In addition, the correlation between the hyperintensities on the MR images and histologic findings was investigated.

Methods

We retrospectively analyzed serial MR images in six autopsy-proved sporadic pCJD cases. The clinical and pathologic findings of the cases are summarized in Table 1. MR images were obtained 3–11 times in each case, 9 days to 29 months after onset. The interval between the first and the last MR examination ranged from 8 months to 29 months. MR imaging studies were performed by using a 0.5-T system or a 1.5-T system. In all cases, axial spin-echo (SE) T1-weighted images (TR/TE, 300–592/14–22; section thickness/intersection gap, 5–7/1–1.5) and axial SE or fast SE (FSE) T2-weighted images (TR/TE, 2800–5000/90–120; section thickness/intersection gap, 5–7/1–1.5) were obtained. In three cases (1, 3, and 5), axial FLAIR images (TR/TE/TI, 6000–8000/110–150/1900–2000; section thickness/intersection gap, 5–7/2–3) were obtained. Evaluation of MR images on DWI was not performed, because the images were available for only one case (6). In three cases (1, 3, and 5), MR images of the formalin-fixed brains (postmortem MR images) were also obtained. The fixed brains were positioned in a standard way in the head coil and axial and coronal FSE T2-weighted images (TR/TE, 3500/96; section thickness/intersection gap, 4/1) were obtained.

The sensitivity of FLAIR imaging in depicting gray matter and white matter lesions is superior or at least equal to that of T2-weighted imaging. In our three cases, in which FLAIR images were obtained, lesions showing hyperintensities on FLAIR images also showed hyperintensities on T2-weighted images, although not as conspicuously as those on FLAIR images (Fig 1). Therefore, in this study, we evaluated the T2 prolongation of lesions on T2-weighted images. As a representative area of the gray matter, we evaluated changes in signal intensity of T2-weighted images of the basal ganglia, because signal intensity in the cerebral cortex is susceptible to the partial volume artifact with the neighboring CSF (Fig 1). Therefore, the conspicuity of hyperintensities of the basal ganglia on T2-weighted images, the degree of cerebral atrophy on T1-weighted images, and the extent of hyperintense areas in the cerebral white matter on T2-weighted images were chronologically assessed independently by two neuroradiologists (S.S., S.F.) without previous knowledge of clinical and pathologic information. The degree of cerebral atrophy was graded into four stages: 0, none; 1, slight; 2, moderate; and 3, severe. The conspicuity of T2 hyperintensities in the basal ganglia was graded as follows: 1, slight (slightly increased signal intensity); 2, moderate (the degree of the conspicuity is between 1 and 3); and 3, severe (isointensity to CSF). The extent of T2 hyperintensities of the white matter was graded as follows: 1, slight (hyperintense areas are confined around the anterior or posterior or both horns of the lateral ventricles); 2, moderate (those extending from the periventricular region to the deep white matter); and 3, severe (diffuse hyperintensities, including subcortical white matter in the cerebral white matter). Hyperintense areas in the brain stem and middle cerebellar peduncle on the T2-weighted images were also evaluated. Evaluation of hyperintensities in the cerebellar white matter and medulla oblongata was excluded in this study.

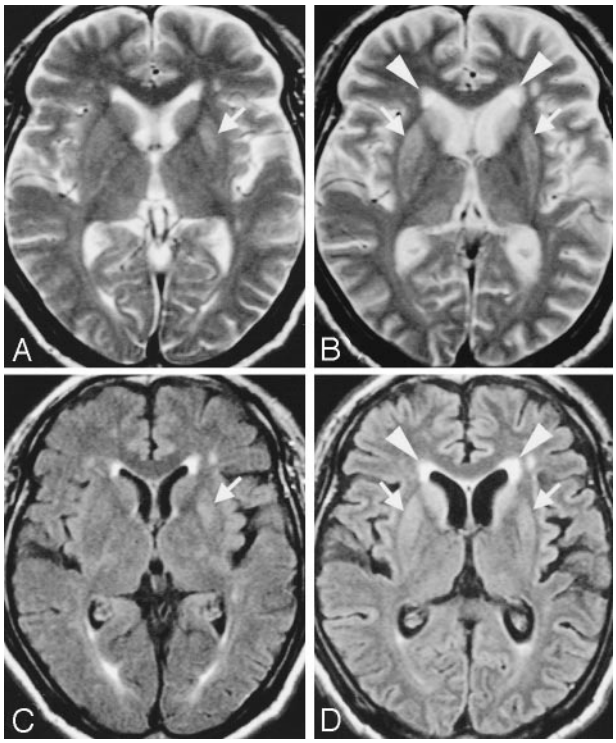

FIG 1. Serial axial T2-weighted (*A* and *B*) and FLAIR (*C* and *D*) images in case 1 obtained 2 (*A* and *C*) and 4 (*B* and *D*) months after onset of symptoms. FLAIR and T2-weighted images show faint hyperintensity in the left putamen. The finding is more conspicuous on the FLAIR image (*C, arrow*) than on the T2-weighted image (*A, arrow*). FLAIR image shows hyperintensities not only in the bilateral striatum (*D, arrows*) and cerebral cortices, but also in the periventricular white matter (*D, arrowheads*) with mild cerebral atrophy 4 months after onset. T2-weighted images also show hyperintensities in both the striatum (*B, arrows*) and periventricular white matter (*B, arrowheads*), although not as conspicuously as on FLAIR images 4 months after onset. Signal intensity in the cerebral cortex is susceptible to the partial volume artifact with the surrounding CSF on T2-weighted images (*A* and *B*).

Neuropathologic examination, including prion protein immunohistochemistry, was performed in all cases, and histologic findings were compared to the last MR images in each case and to the postmortem MR images in three cases.

Results

Serial Changes of MR Images

Serial changes in the conspicuity of hyperintensities of the cerebral basal ganglia, the degree of cerebral atrophy, and the extent of hyperintensities in the cerebral white matter, as well as in the brain stem and middle cerebellar peduncle, in each case are summarized in Table 2, which can be accessed at www.ajnr.com.

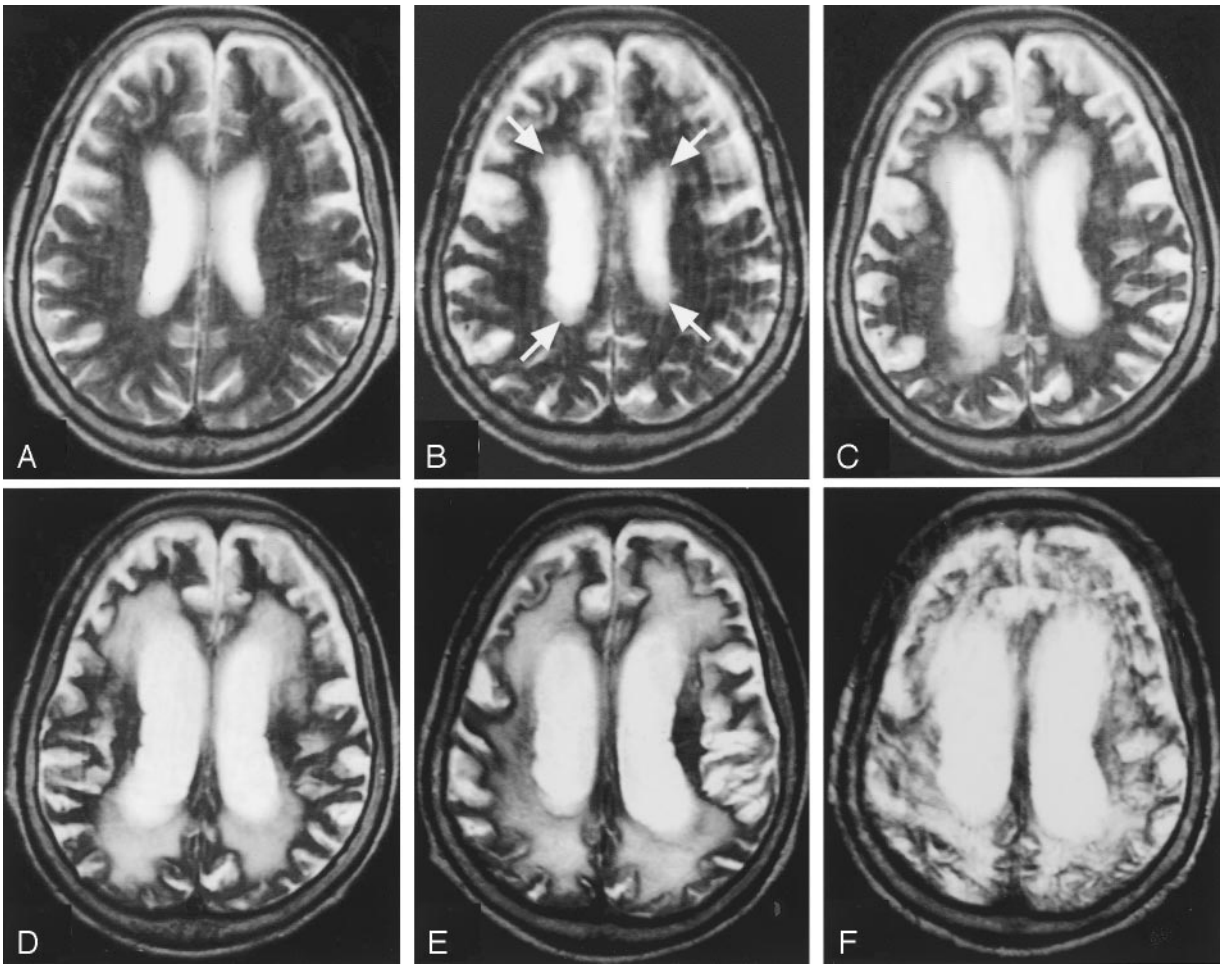

FIG 2. Serial axial T2-weighted MR images from case 4 obtained (*A*) 3 months, (*B*) 5 months, (*C*) 7 months, (*D*) 9 months, (*E*) 12 months, and (*F*) 18 months after onset of symptoms. Slight hyperintensities are shown around the lateral ventricles (*B, arrows*) 5 months after the onset. The periventricular hyperintensities are gradually extending to the deep and subcortical white matter in parallel with cortical atrophy (*C– F*).

T2 hyperintensities of the basal ganglia were seen 2–5 months after the onset of symptoms, at the same time as the appearance of the hyperintensities in the cerebral white matter in one case (3) and 2–4 months earlier than the appearance of the hyperintensities in the cerebral white matter in four cases (1, 2, 4, and 5) (Fig 1). In case 5, the conspicuity of the hyperintensities became more prominent sequentially, whereas the conspicuity in cases 1–4 remained mild during the entire clinical course. T2 hyperintensities of the cerebral white matter were first noted in the periventricular region 4–5 months after onset in cases 1, 3, and 4 (Figs 1 and 2), at approximately the same time as cortical atrophy was seen. Five to 9 months after the onset of symptoms, the T2 hyperintensities extended from the periventricular white matter to the deep white matter, partially to the subcortical white matter and progressed to a severe degree from 10 months after the onset of symptoms (Fig 2).

T2 hyperintensities were also seen in the bilateral corticospinal tracts in cases 5 and 6 at 15 and 18 months after the onset of symptoms, respectively, which subsequently became more prominent (Fig 3). From 19 months after the onset of symptoms, T2 hyperintensities also became apparent in the pontine base and middle cerebellar peduncles in cases 3, 5, and 6 (Fig 3).

Histologic Findings of the Brain

In all cases except 1, degenerative changes represented by spongiform change, neuronal loss, and proliferation of hypertrophic or gemistocytic astrocytes were severe in the cerebral neocortices and moderate to severe in the basal ganglia and thalamus. The cerebral white matter showed severe loss of myelin and axons associated with spongiform changes or tissue rarefaction, numerous foamy macrophages, and proliferation of gemistocytic astrocytes. In case 1, degenerative changes were moderate in the cerebral neocortices, basal ganglia, and thalamus. In the brain stem, neuronal loss and gliosis were mild to moderate in cases 2–4 and severe in cases 5 and 6. In case 1, the brain stem was well preserved. Loss of myelin and axons with macrophage infiltration and fibrillary gliosis, compatible with secondary degeneration, in the corticospinal tracts in the internal capsule and brain stem were mild in cases 2 and 4, moderate in case 3,

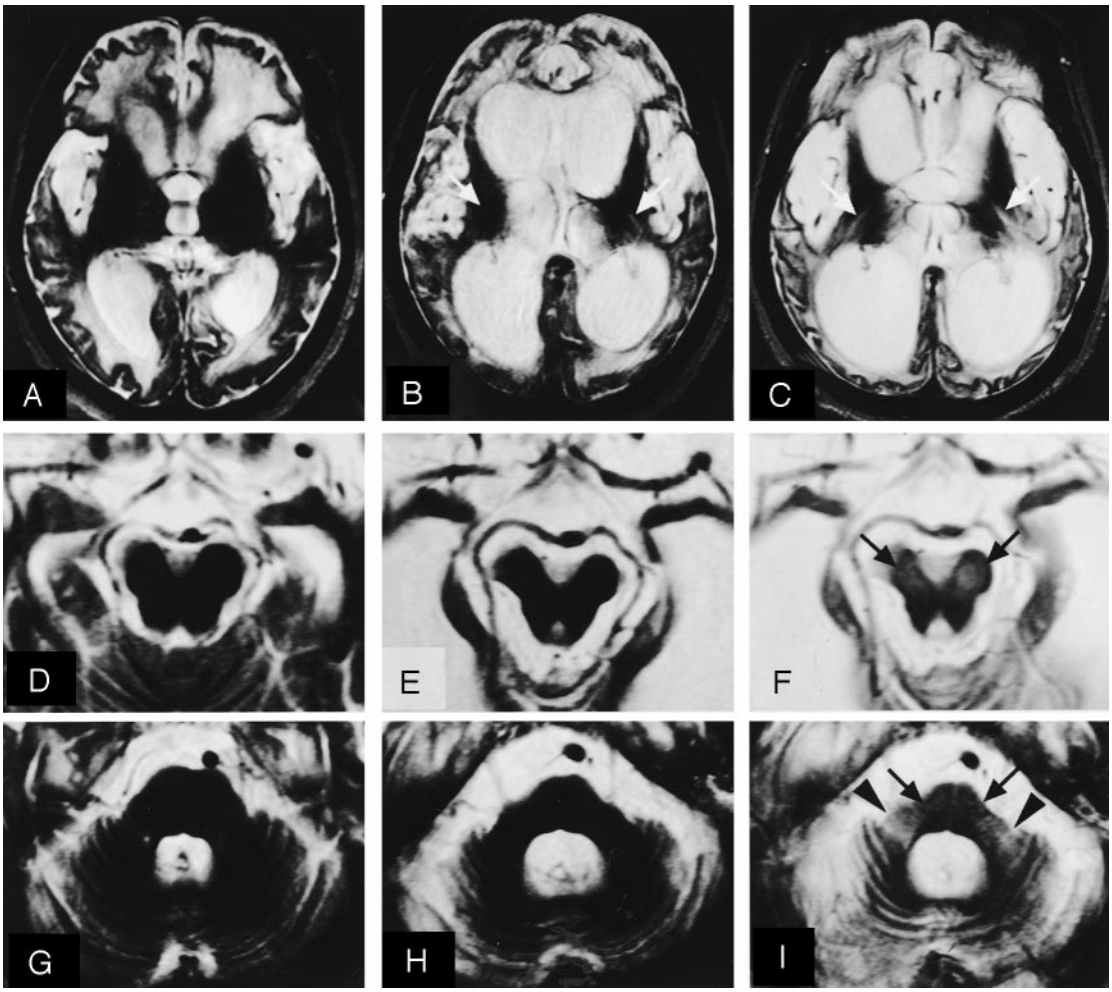

FIG 3. Serial axial T2-weighted MR images in case 6 obtained at 11 months (*A, D,* and *G*), 18 months (*B, E,* and *H*), and 28 months (*C, F,* and *I*) after the onset of symptoms. The degree of brain atrophy gradually becomes apparent. Only in this case, T2 hyperintensities are never seen in the basal ganglia at any stage. At 11 months after onset, diffuse T2 hyperintensities in the cerebral white matter are evident, but hyperintensities are not visible in the internal capsules (*A*). At 18 months, T2 hyperintensities are observed in both internal capsules (*B, arrows*). At 28 months, high signal intensity of the bilateral internal capsules is apparent (*C, arrows*). T2 hyperintensities are also visible in both cerebral peduncles (*F, arrows*), pons (*I, arrows*), and middle cerebellar peduncles (*I, arrowheads*).

and severe in cases 5 and 6. Similar features were also found in the middle cerebellar peduncles: mild in case 4, moderate in case 3, and severe in cases 5 and 6. Prion protein immunohistochemistry revealed a diffuse synaptic type of deposition in the gray matter in all cases.

Histologic Features of Hyperintense Areas in the White Matter

The cerebral white matter in five of the six cases revealed histologically severe loss of myelin and axons associated with spongiform changes or tissue rarefaction, numerous macrophages, and proliferation of gemistocytic astrocytes.

In the present study, postmortem MR images were obtained in cases 1, 3, and 5. In cases 3 and 5, with 22 and 28 months of the clinical course, respectively, the extent of cerebral white matter lesions on the postmortem T2-weighted images (Fig 4A) was the same as that obtained by histologic examination (Fig 4B). The area of highly increased signal intensity (Fig 4A) revealed histologically severe loss of myelin and axons associated with severe spongiform changes or tissue rarefaction and proliferation of gemistocytic astrocytes (Fig 4B and C). By contrast, the area of moderately increased signal intensity (Fig 4A) showed mild to moderate spongiform changes or tissue rarefaction (Fig. 4B and D). In case 1, with the shortest clinical course (8 months), cerebral white matter lesions were visible as areas of moderately increased signal intensity. The extent was mild to moderate on the postmortem T2-weighted images (Fig 5A) but more extensive on the myelin-stained sections (Fig 5B). Histologic features of the lesions were the same in nature as those in cases 3 and 5, but the degree of spongiform changes or tissue rarefaction was mild (Fig 5C). The area of normal signal intensity (Fig 5A) showed no apparent degenerative changes (Fig 5B and D).

The corticospinal tracts seen as T2 hyperintensities in the internal capsules, the cerebral peduncles (Fig

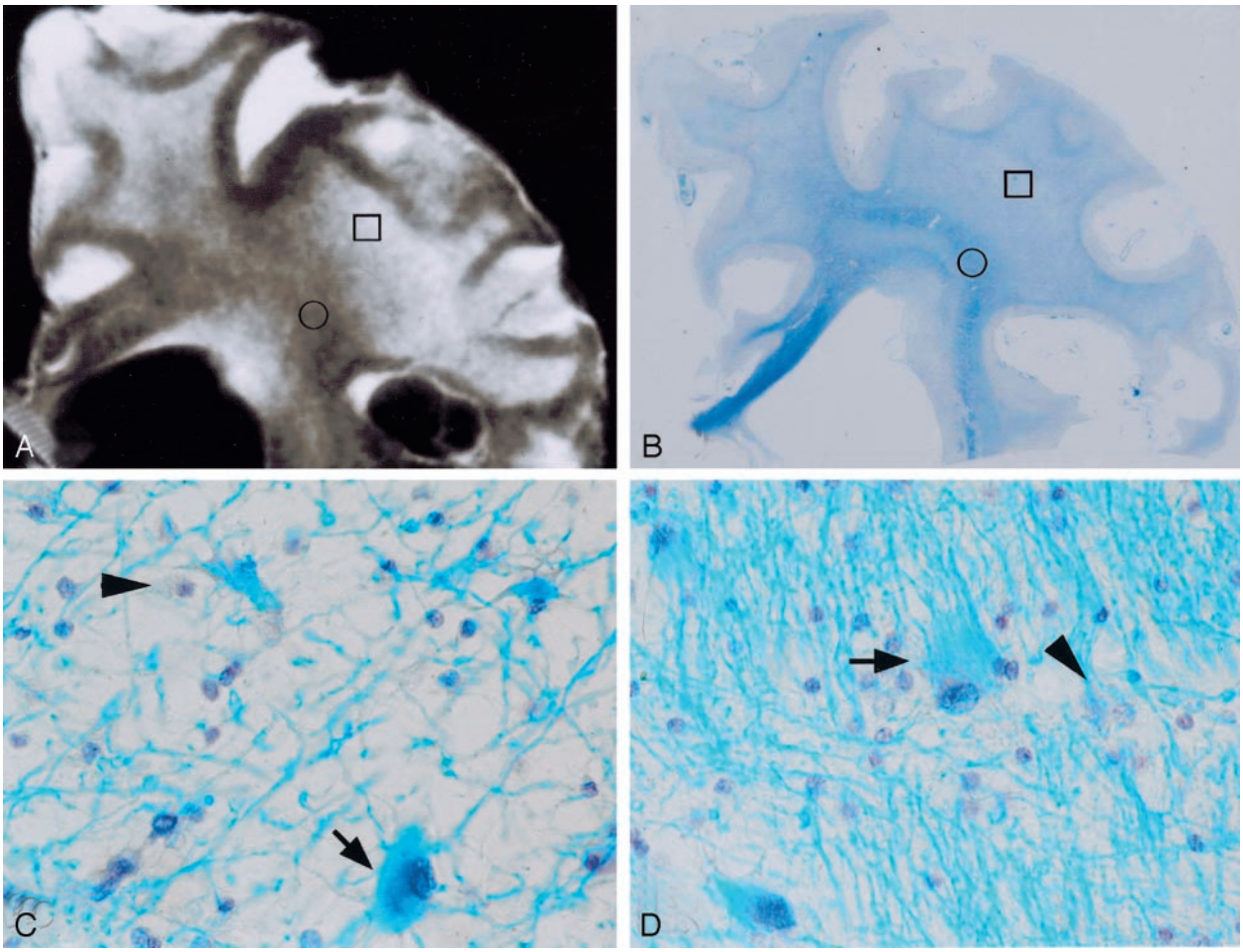

FIG 4. *A,* Postmortem coronal T2-weighted image of the right frontal lobe 22 months after the onset in case 3, showing diffuse hyperintensities in the cerebral white matter. *B,* Myelin-stained section corresponding to panel *A,* demonstrating diffuse pallor of the cerebral white matter. *C,* Histologic specimen of the area of highly increased signal intensity (*A* and *B, squares*), revealing a severe loss of myelin and axons, tissue rarefaction, foamy macrophages (*arrowhead*), and proliferation of gemistocytic astrocytes (*arrow*). *D,* Area of moderately increased signal intensity (*A* and *B, circles*), showing mild tissue rarefaction. There are also foamy macrophages (*arrowhead*) and gemistocytic astrocytes (*arrow*). Because tissue rarefaction and gemistocytic astrocytosis are exceptional features in secondary degeneration, these histologic features indicate primary involvement of the white matter.

6A) and the longitudinal fasciculi in the pontine base (Fig 6B) in cases 5 and 6 showed a severe loss of myelin and axons with moderate macrophage infiltration and fibrillary gliosis (Figs 6C and E), characteristics compatible with secondary degeneration. Hyperintense areas in the pontine base and middle cerebellar peduncles in cases 3 and 5 (Fig 6B), and 6 revealed neuronal loss and proliferation of hypertrophic astrocytes in the pontine nuclei (Figs 6D and F) and secondary degeneration of the pontine transverse fibers and middle cerebellar peduncles (Figs 6D and G).

Discussion

White matter lesions of pCJD demonstrated as T2-prolonged areas have been considered secondary changes to cortical lesions of pCJD (30), although autopsy studies have suggested that the lesions are primary changes of the disease, like those in the gray matter (5, 8–10, 12–15). We evaluated white matter lesions of pCJD by chronological MR images and MR-pathologic correlations to elucidate whether the white matter lesions are primary or secondary degeneration. In 1990, Kruger et al (7) first reported T2 hyperintensities in the periventricular white matter in the later stages of an autopsy-proved case of pCJD. In 1991, Uchino et al (18) reported MR images in two autopsy-proved cases of pCJD and described mild cerebral atrophy and periventricular white matter degeneration appearing 5 and 6 months after the onset of symptoms, which became more widespread 17 and 14 months after onset, 8 and 6 months before death, respectively. In the present study, serial MR images of the brains affected by pCJD revealed that T2 hyperintensities appeared in the cerebral gray matter 2–5 months after the onset of symptoms. T2 hyperintensities were not found in the cerebral white matter within 3 months after disease onset in three cases examined. The T2 hyperintensities first appeared in the periventricular white matter 4–5 months after the onset in cases 1, 3, and 4, at approximately the same time that cortical atrophy was seen. Five to 9 months after onset, the T2 hyperintensities extended from the periventricular white matter to the deep white matter,

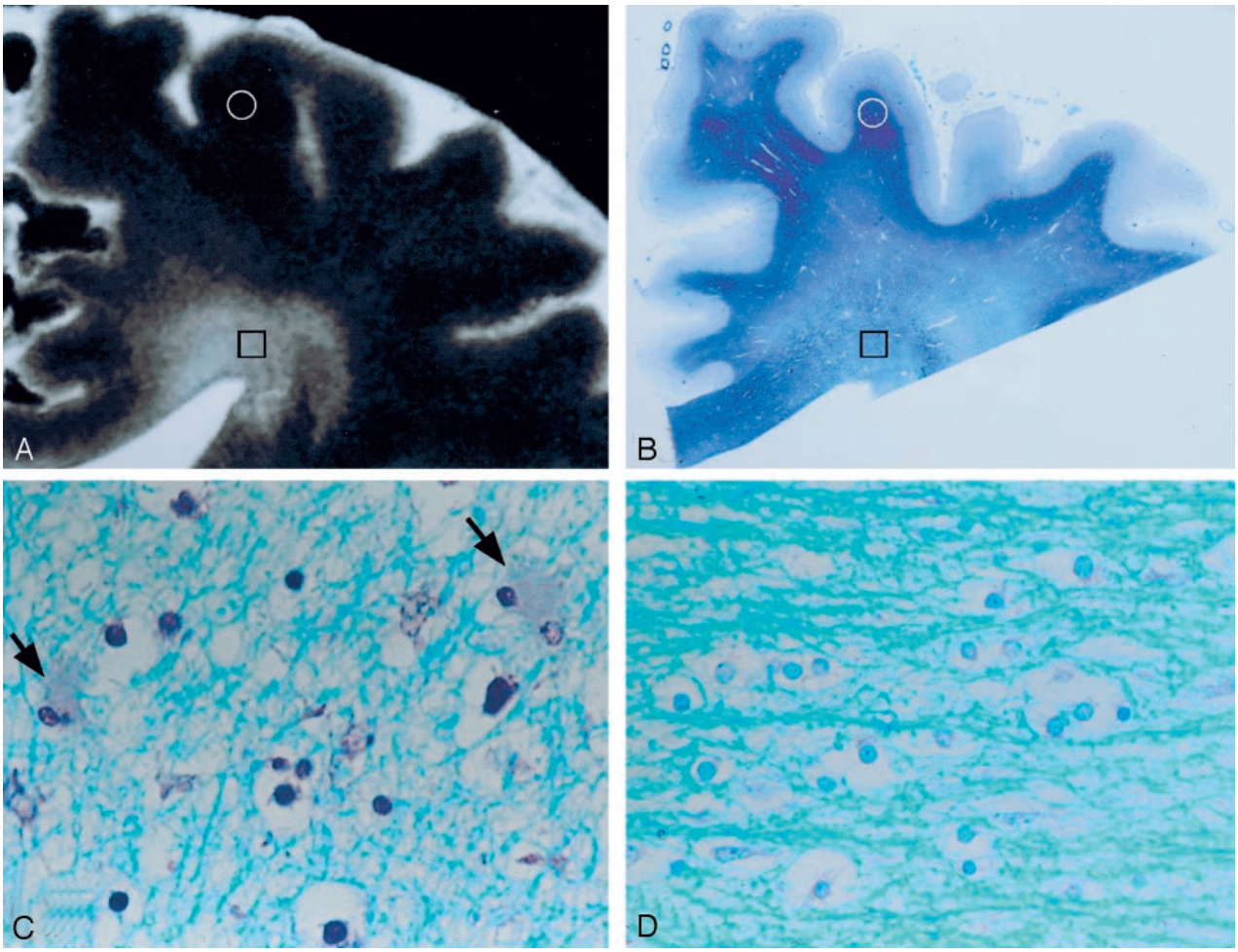

FIG 5. *A,* Postmortem coronal T2-weighted image of the right frontal lobe 8 months after the onset of symptoms in case 1, showing hyperintensities around the anterior horn of the lateral ventricle and adjacent deep cerebral white matter. *B,* Myelin-stained section corresponding to panel *A,* showing pallor of the cerebral white matter, which is more widespread than the extent of hyperintensities on the MR image. *C,* Histologic specimen of the area of moderately increased signal intensity (*A* and *B, squares*), revealing mild loss of myelin and axons with a few hypertrophic astrocytes (*arrows*). *D,* Area of normal signal intensity (*A* and *B, circles*), showing no apparent degenerative changes.

partially to the subcortical white matter, and progressed to a severe degree from 10 months after the onset. This pattern of the extension of cerebral white matter lesions as shown on MR images would suggest that the white matter lesions are not secondary to cortical lesions but primary lesions of the disease.

The cerebral white matter in five of six cases revealed a histologically severe loss of myelin and axons accompanied by spongiform changes or tissue rarefaction, numerous macrophages, and proliferation of gemistocytic astrocytes. These findings are characteristic of the cerebral white matter lesions of pCJD. Histologic features of the cerebral white matter in case 1, which had the shortest clinical course, were the same in nature as those of the other cases, except for a mild degree of spongiform changes or tissue rarefaction. Since both spongiform changes and gemistocytic astrocytosis are exceptional features of secondary degeneration, these histologic features indicate primary involvement of the white matter (5, 8–10, 12–15). Therefore, cerebral white matter lesions in the cases here are considered to be primary changes of the disease on the basis of histologic features and the pattern of the extension of the cerebral white matter lesions on the MR images.

Comparison of the postmortem MR images of cerebral white matter with their histologic findings in the three cases examined revealed the extent of T2 hyperintensities to be the same as the histologic results in the cases with a longer clinical course or with severe histologic changes. They were less widespread, however, in those cases with a shorter clinical course or with mild histologic changes. It was also demonstrated that the degree of signal intensity reflected the severity of histologic changes in the cerebral white matter, particularly in spongiform changes or tissue rarefaction.

The present MR imaging study first demonstrated the occurrence of T2 hyperintensities in the bilateral corticospinal tracts in the internal capsule and brain stem in two cases, although their signal intensity was less than that of the other cerebral white matter. The findings appeared at later stages in both cases, 15 and 18 months after the onset, respectively, when the degree of brain atrophy and the extent of T2 hyper-

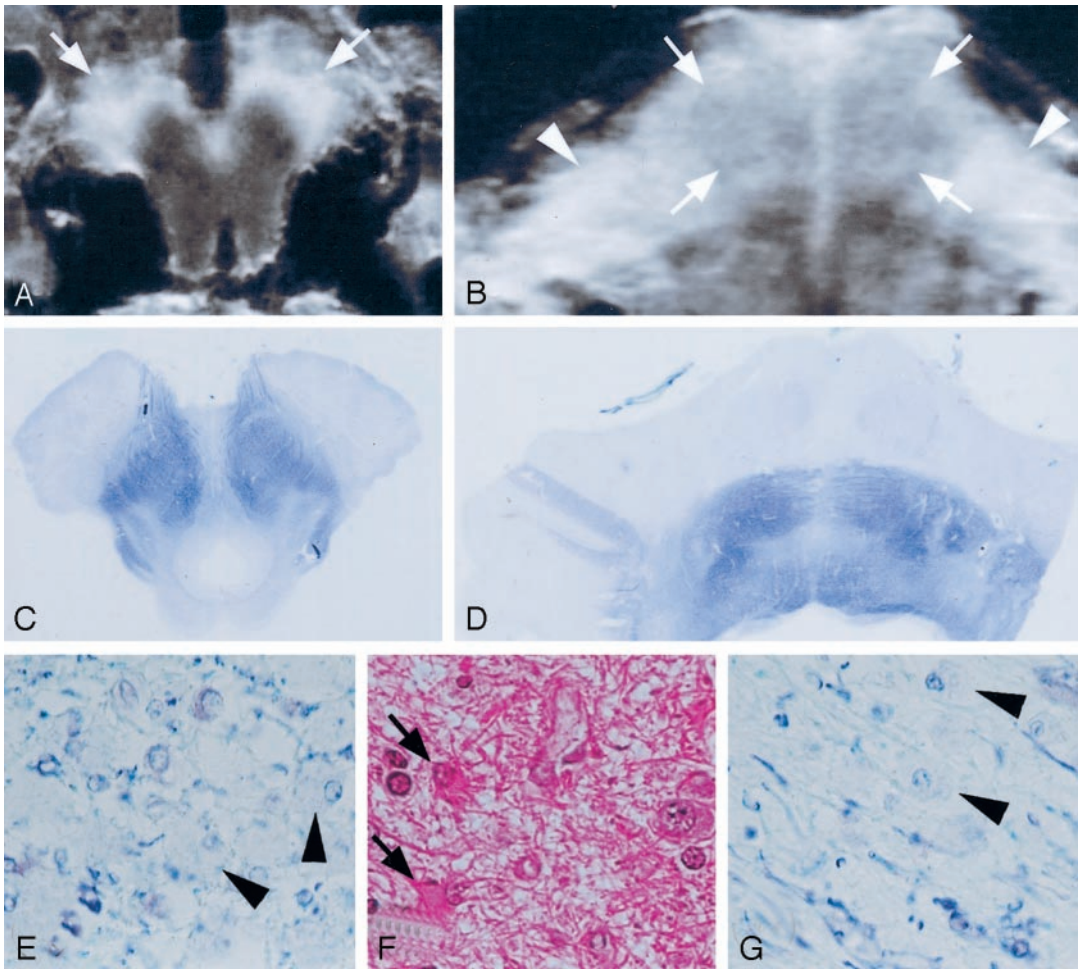

FIG 6. *A* and *B*, Postmortem axial T2-weighted images of the midbrain (*A*) and pons (*B*) 28 months after the onset of symptoms in case 5, showing hyperintensities in the cerebral peduncles (*A, arrows*), pons (*B, arrows*), and middle cerebellar peduncles (*B, arrowheads*) involving the longitudinal fasciculi, pontine nuclei, and pontine transverse fibers. *C* and *D*, The myelin-stained sections corresponding to panels *A* and *B* demonstrate severe pallor of the cerebral peduncles (*C*), pons, and middle cerebellar peduncles (*D*). *E,* Histologically, the cerebral peduncle shows severe loss of myelin and axons with moderate macrophage infiltration (*arrowheads*) and fibrillary gliosis, characteristics compatible with secondary degeneration. *F,* Pontine nuclei reveal neuronal loss and proliferation of hypertrophic astrocytes (*arrows*). *G,* Middle cerebellar peduncle shows severe loss of myelin and axons with moderate macrophage infiltration (*arrowheads*) but no gemistocytic astrocytes, a characteristic compatible with secondary degeneration.

intensities in the cerebral white matter had already reached a severe degree. Accordingly, it was suggested that the lesions of the corticospinal tracts might be secondary to the cortical or cerebral white matter lesions. Furthermore, histologic examination of the corticospinal tracts in the internal capsule and brain stem revealed a loss of myelin and axons accompanied by mild infiltration of macrophages and fibrillary gliosis, which differed from that of the other white matter lesions wherein spongiform changes or tissue rarefaction were always accompanied by proliferation of gemistocytic astrocytes. These results support that the lesions of the corticospinal tracts in the internal capsule and brain stem are secondary to motor cortex or cerebral white matter lesions.

To our knowledge, there has been only one imaging study of pCJD describing the CT findings of hypoattenuated areas in the pontine base and middle cerebellar peduncles at the terminal stage of one patient with a clinical course of 40 months (16). Some autopsy studies of pCJD, however, have described degeneration of the pontine nuclei or middle cerebellar peduncles or both in cases with long clinical course (4, 11, 12, 15, 16, 22). In the present study, T2 hyperintensities were also noted in the pontine base and middle cerebellar peduncles at the terminal stages of three cases with long clinical courses. Histologic examination disclosed neuronal loss and mild spongiform changes by gemistocytic astrocytosis in the pontine nuclei and degeneration of the transverse pontine fibers and middle cerebellar peduncles accompanied by fibrillary gliosis. These findings indicate that the lesions of the pontine nuclei are primary, but that those of the pontine transverse fibers and middle cerebellar peduncles are secondary to the pontine nuclei lesions.

All cases in this study had clinical histories of rapidly progressive dementia, followed by myoclonus and akinetic mutism, and showed periodic synchronous discharge on EEG. Akinetic mutism appeared 2–4

months after the onset in all cases except 6. MR images revealed that T2 hyperintensities appeared in the cerebral gray matter 2–5 months after the onset of symptoms. On the other hand, white matter lesions first appeared 4–5 months after onset around the lateral ventricles and became severe 10 months after the onset in all cases. These findings suggest that akinetic mutism in pCJD is mainly due to the cerebral cortical lesions.

Conclusion

The present MR imaging and histologic study of pCJD demonstrates that T2 hyperintensities appeared in the cerebral gray matter 2–5 months after the onset of symptoms and that T2 hyperintensities of cerebral white matter first appeared around the lateral ventricles 4 to 5 months after onset and rapidly extended first to the deep or subcortical white matter during the following several months and then throughout the cerebral white matter from 10 months after onset. There was a good correlation between the degree of signal intensity on the T2-weighted images and the severity of histologic changes in the cerebral white matter. Both the pattern of the extension of T2 hyperintensities in the cerebral white matter on the MR images and their histologic features indicated that cerebral white matter lesions in pCJD were primary changes of the disease. In addition, the present study describes the occurrence of T2 hyperintensities in the corticospinal tracts in the internal capsule and brain stem at a later stage of the disease, which were considered secondary to the cerebral cortical or white matter lesions or both.

References

1. Gonatas NK, Terry RD, Weiss M. **Electron microscopic study in two cases of Creutzfeldt-Jakob disease.** *J Neuropathol Exp Neurol* 1965;24:575–598
2. Lampert PW, Gajdusek DC, Gibbs CJ. **Subacute spongiform virus encephalopathies.** *Am J Pathol* 1972;68:626–646
3. Park TS, Kleinman GM, Richardson EP. **Creutzfeldt-Jakob disease with extensive degeneration of white matter.** *Acta Neuropathol* 1980;52:239–242
4. Monreal J, Collins GH, Masters CL, et al. **Creutzfeldt-Jakob disease in an adolescent.** *J Neurol Sci* 1981;52:341–350
5. Macchi G, Abbamondi AL, Di Trapani G, et al. **On white matter lesions of the Creutzfeldt-Jakob disease.** *J Neurol Sci* 1984;63:197–206
6. Kovanen J, Erkinjuntti T, Iivanainen M, et al. **Cerebral MR and CT imaging in Creutzfeldt-Jakob disease.** *J Comput Assist Tomogr* 1985;9:125–128
7. Kruger H, Meesmann C, Rohrback E. **Panencephalopathic type of Creutzfeldt-Jakob disease with primary extensive involvement of white matter.** *Eur Neurol* 1990;30:115–119
8. Cruz-Sanchez FF, Ferrer I, Rossi ML. **On the white matter changes in spongiform encephalopathy.** *Dementia* 1991;2:106–111
9. Carota A, Pizzolato GP, Gailloud P, et al. **A panencephalopathic type of Creutzfeldt-Jakob disease with selective lesions of the thalamic nuclei in 2 Swiss patients.** *Clin Neuropathol* 1996;15:125–134
10. Mizutani T, Okumura A, Oda M, et al. **Panencephalopathic type of Creutzfeldt-Jakob disease: primary involvement of the cerebral white matter.** *J Neurol Neurosurg Psychiatry* 1981;44:103–115
11. Tateishi J, Ohta M, Koga M, et al. **Transmission of chronic spongiform encephalopathy with Kuru plaques from humans to small rodents.** *Ann Neurol* 1979;5:581–584
12. Riku S, Okamoto T, Hashizume Y, et al. **Panencephalopathic type of Creutzfeldt-Jakob disease and special reference to its pyramidal tract degeneration.** *Clin Neurol* 1983;23:147–151
13. Ueda N, Miyazaki K, Imai S, et al. **Creutzfeldt-Jakob disease: an autopsy case of the panencephalopathic type and a review of the literature.** *Acta Pathol Jpn* 1985;35:1483–1494
14. Tobo M, Tashiro T, Fujii I, et al. **Creutzfeldt-Jakob disease with extensive white matter involvement.** *Neurol Med* 1985;23:342–349 [in Japanese]
15. Okiyama R, Tsuchiya K, Furukawa T, et al. **An autopsy case of panencephalopathic type of Creutzfeldt-Jakob disease: an early clinical sign documented by magnetic resonance imaging.** *Clin Neurol* 1989;29:1048–1051
16. Yagishita A. **Computed tomography of Creutzfeldt-Jakob disease.** *Jpn J Clin Radiol* 1989;34:1317–1325 [in Japanese]
17. Mori S, Hamada C, Kumanishi T, et al. **A Creutzfeldt-Jakob disease agent (Echigo-1 strain) recovered from brain tissue showing the "panencephalopathic type" disease.** *Neurology* 1989;39:1337–1342
18. Uchino A, Yoshinaga M, Shiokawa O, et al. **Serial MR imaging in Creutzfeldt-Jakob disease.** *Neuroradiology* 1991;33:364–367
19. Sasaki A, Hirato J, Nakazato Y. **Immunohistochemical study of microglia in the Creutzfeldt-Jakob diseased brain.** *Acta Neuropathol* 1993;86:337–344
20. Aoki T, Kobayashi K, Isaki K. **Microglial and astrocytic change in brains of Creutzfeldt-Jakob disease: an immunocytochemical and quantitive study.** *Clin Neuropathol* 1999;18:51–60
21. Tanaka S, Saito M, Morimatsu M, et al. **Immunohistochemical studies of the PrP deposition in Creutzfeldt-Jakob disease.** *Neuropathology* 2000;20:124–133
22. Konagawa M, Sakai M, Asakura K, et al. **T2-weighted MRI and pathological findings in the cerebral hemisphere of panencephalitic Creutzfeldt-Jakob disease.** *Brain Nerve* 2001;53:398–399 [in Japanese]
23. Gertz H-J, Henkes H, Cervos-Navarro J. **Creutzfeldt-Jakob disease: correlation of MRI and neuropathologic findings.** *J Neurol* 1988;38:1481–1482
24. Finkenstaedt M, Szudra A, Zerr I, et al. **MR imaging of Creutzfeldt-Jakob disease.** *Radiology* 1996;199:793–798
25. Schroter A, Zerr I, Henkel K, et al. **Magnetic resonance imaging in the clinical diagnosis of Creutzfeldt-Jakob disease.** *Arch Neurol* 2000;57:1751–1757
26. Schwaninger M, Winter R, Hacke W, et al. **Magnetic resonance imaging in Creutzfeldt-Jakob disease: evidence of focal involvement of the cortex.** *J Neurosurg Psychiatry* 1997;63:408–409
27. Demaerel P, Baert AL, Vanopdenbosch L, et al. **Diffusion-weighted magnetic resonance imaging in Creutzfeldt-Jakob disease.** *Lancet* 1997;349:847–848
28. Bahn MM, Kido DK, Lin W, et al. **Brain magnetic resonance diffusion abnormalities in Creutzfeldt-Jakob disease.** *Arch Neurol* 1997;54:1411–1415
29. Mittal S, Farmer P, Kalina P, et al. **Correlation of diffusion-weighted magnetic resonance imaging with neuropathology in Creutzfeldt-Jakob disease.** *Arch Neurol* 2002;59:128–134
30. Tzeng B-C, Chen C-Y, Lee C-C, et al. **Rapid spongiform degeneration of the cerebrum and cerebellum in Creutzfeldt-Jakob disease.** *AJNR Am J Neuroradiol* 1997;18:583–586